J Mol Model (2015) 21:20
DOI 10.1007/s00894-014-2566-0

ORIGINAL PAPER

Computational study of interaction of alkali metals with C_3N nanotubes

Farzad Molani · Seifollah Jalili · Jeremy Schofield

Received: 30 August 2014 / Accepted: 14 December 2014

Abstract Interaction of the alkali metals (AMs) like lithium (Li), sodium (Na), and potassium (K) with defective and non-defective (8,0) C_3N nanotubes (C_3NNT) have been investigated using the first-principles study. In addition to structural properties, we have also studied the electronic properties, charge transfer, and work function of the AM-C_3NNT complexes. AMs are adsorbed on hollow sites, regardless of the initial positions. Upon the adsorption of AMs, the structures exhibit semiconducting behavior. Furthermore, interaction of Li atom can be explained by Dewar model, whereas for the other atoms there are different explanations. For all metal adsorbates, the direction of the charge transfer is from adsorbate to adsorbent, because of their high surface reactivity. The results showed that the nanotube with carbon vacancy is the most favorite adsorbent. Our findings also indicated that the enhancement in absolute adsorption energy is in order of Li > K > Na. It is noteworthy that clustering of AM atoms on the nanotubes with and without defects is not expected. It is worthy that C_3NNT is a better adsorbent for AM atoms than CNT, graphene, C_{60}, and B_{80}.

F. Molani (✉)
Department of Chemistry, Sanandaj Branch, Islamic Azad University, P. O. Box 618, Sanandaj, Iran
e-mail: f.molani@iausdj.ac.ir

S. Jalili
Department of Chemistry, K. N. Toosi University of Technology, P. O. Box 15875-4416, Tehran, Iran

S. Jalili
Computational Physical Sciences Research Laboratory, School of Nano-Science, Institute for Research in Fundamental Sciences (IPM), P.O. Box 19395-5531, Tehran, Iran

J. Schofield
Chemical Physics Theory Group, Department of Chemistry, University of Toronto, 80 Saint George Street, Toronto, ON M5S 3H6, Canada

Published online: 27 January 2015

Keywords Alkali metal · C_3N nanotube · Density functional theory · Vacancy defect · Electronic properties

Introduction

The adsorption of AMs (highly reactive chemical species) on the nanostructure surfaces have been widely studied for several applications such as substantial activity in gasification reactions [1], improved gas sensing of the substrate [2–4], and rechargeable batteries [5, 6]. Furthermore, AMs have good thermal and electrical conductivity; however, the doping of the nanotubes with these metals has been hardly discussed. Thus, investigation of adsorption of these atoms on new nanomaterials seems to be necessary. Chemical doping with foreign atoms is an effective method to modify the properties of the host materials. Among them, nitrogen doping plays a critical role in regulating the electronic properties of the carbon materials. Because of significant changes in metal adsorption, the electro-catalytic activity for reduction of oxygen and H_2O_2, fast direct electron transfer kinetics for glucose oxidase, hardness, and electrical conductivity [7–13], substitution of doping of nitrogen atom has received attention. This indicates that N-doped carbon nanostructures are promising candidates for applications in surfaces, nano-electronic, electrochemical energy devices (fuel cells, metal–air batteries), and biosensors [5, 8–10, 14–18].

After CN_x nanotubes were synthesized [19], some theoretical studies were done [20–22]. The studies have shown that the C_3NNT exhibits a distorted structure that is strongly independent of the chiral index [20, 22]. Some predictions of the possible crystal structures for C_3N can be found in the literature [22, 23]. Since C–N bonds are more favorable than C–B

bonds [24], the C_3N nanotube is more stable than the BC_3 one. Recently, the effect of defects on the structural and electronic properties of C_3NNT has been studied [21]. When a single atom is removed from the C_3NNT sidewall, unconstrained structure optimization leads to the formation of a new bond, perpendicular to the tube axis and the system is reconstructed to a five-membered and a nine-membered ring with a dangling bond or under-coordinated atom (UA) around the local defect region. Moreover, the study has shown that, the carbon vacancy (C_v) defect is more stable than the nitrogen vacancy (N_v) defect [21].

Therefore, motivated by such perspective, in the present contribution we have investigated the structural and electronic properties of defective and non-defective C_3NNT with AM atoms as a new material for future technologies.

Computational details

Spin-polarized DFT calculations were carried out using the Quantum Espresso package (version 4.3.2) [25] with the exchange-correlation potential described by Perdew–Zunger [26] of the local density approximation (LDA). We have also compared the LDA results with those from generalized gradient approximation (GGA) with the Perdew-Burke-Ernzerhof functional [27]. It is well-known that the accurate adsorption energy is typically in between the GGA and LDA values. Note that the energy values in parenthesis are related to GGA calculations. Furthermore, ultrasoft pseudopotential for a description of interaction was used [28]. The energy cutoff for the plane-wave basis set was taken to be 600 eV. To explicitly study the interaction between (8,0) C_3NNT and AMs, we employed a periodically repeating tetragonal supercell of 20 Å×20 Å×17.08 Å, containing 128 atoms for the perfect C_3NNT and one AM. The length of c equal to four the periodicity of the (8,0) C_3NNT. This value was obtained by optimization of cell parameters upon total energy. Distance of the metal adjacent images in z-axis is about 17.08 Å. So, with a good approximation, we can conclude that the c parameter is suitable. Furthermore, a large supercell parameter of 20 Å was chosen in x and y directions to ensure negligible interaction between the system and its images in neighboring cells. The Brillouin-zone integration was performed with a 1×1×9 Monkhorst-Pack k-points mesh [29]. The calculations showed that increasing the k points has little change in the final results. All structures were fully optimized until the forces on each atom were less than 0.01 eV $Å^{-1}$. Furthermore, binding (adsorption) energy was given by $E_b=E_{AM@tube}-E_{AM}-E_{tube}$, where $E_{AM@tube}$, E_{AM}, and E_{tube} are the total energy of AM on corresponding nanotube, total energy of AM, and total energy of corresponding nanotube, respectively. To ensure that the most stable configuration could be achieved, the AM atom was placed at different positions. In order to charge analysis, Löwdin method was used [30]. It is noteworthy that a negative (positive) value for charge transfer (CT) indicates that the AMs lose (gain) charge density. Furthermore, the work function (Φ) is the minimum energy required to extract one electron from the surface to a point in the vacuum [31].

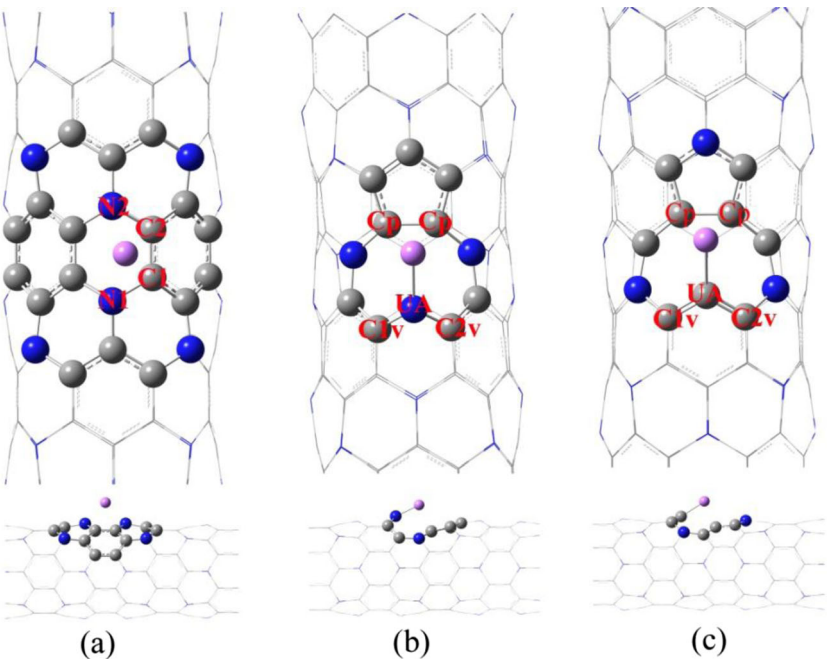

Fig. 1 The optimized structures of Li atom on (**a**) perfect, (**b**) C_v, and (**c**) N_v nanotubes. *Gray*, *blue*, and *pink* colors represent carbon, nitrogen, and lithium atoms, respectively

Table 1 Calculated structural and electronic properties of Li atom on C_3NNT

System	D_{min}(Li-X) (Å)	L (Cp-Cp) (Å)	L (UA-C1v) (Å)	L (UA-C2v) (Å)	E_{gap} (eV)	E_b (eV)	$CT_{(s)}$ |e|	$CT_{(p)}$ |e|	Φ (eV)
Li@perfect	2.066	–	–	–	0.1	−2.60 (−1.26)	−0.87	+0.31	2.03
Li@C_v	1.838	1.463	1.393	1.397	0.12	−4.29 (−3.02)	−0.85	+0.39	2.11
Li@N_v	1.971	1.514	1.378	1.378	0.04	−3.63 (−2.33)	−0.85	+0.40	2.03

Minimum distance of Li atom with nanotube (D_{min}), bond lengths (L), energy gap between valance and conduction bond (E_{gap}), binding energy (E_b), charge transfer of s orbital of Li atom ($CT_{(s)}$), charge transfer of p orbital of Li atom ($CT_{(p)}$), work function (Φ) for Li atom on C_3NNT

Results and discussion

Adsorption of Li atom on C_3NNT

The optimized structures of Li atom on the perfect and defective tubes are shown in Fig. 1. Furthermore, the structural and electronic parameters are listed in Table 1. In the perfect case, Li atom prefers to stay on the hexagon ring consisting of four C atoms and two N atoms (4C-2 N), regardless of the initial positions. Minimum distance (D_{min}) between Li atom with C and N atoms are 2.212 and 2.066 Å, respectively. Bond lengths of C1-C2 and C1-N1 are elongated to 1.419 and 1.459 Å. These elongations are justified by the CT about 0.56 |e| from Li atom to the nanotube. As depicted in Fig. 1, in both defective structures, Li atom prefers to stay on nano-membered ring. From Table 1, the new bonds between Li atom and UA in C_v and N_v structures are about 1.838 and 1.971 Å, respectively. Furthermore, bond lengths around defect region are increased. Like perfect form, Li atom on C_v and N_v nanotubes lost 0.46 and 0.45 |e|, respectively. Moreover, E_b of Li atom on perfect, C_v, and N_v structures are −2.60 (−1.26), −4.29 (−3.02), and −3.63 (−2.33) eV, respectively (as mentioned earlier, values in parenthesis are referred to as GGA approximation). Compared with experimental cohesive energy of Li bulk (1.63 eV/atom) [31], clustering of Li atom on C_3NNT is not expected. Upon the binding energies, C_v structure is the best host material for Li atom. Such a large adsorption energy gain means that newly formed Li-N and Li-C bonds are quite strong. Therefore, Li atom at C_v is characterized with a larger absolute E_b and shorter chemical bonds. Most notably, adsorption energy of Li atom on N-doped CNT is +0.7 eV and endothermic [32], whereas adsorption on the perfect C_3NNT is −2.60 (−1.26) eV and exothermic. Therefore, E_b of Li atom increases as the number of N atom increases. With same approximation, C_3NNT is a better adsorbent as compared to B- and N-doped CNT [32], graphene [33], silicene [34], C_{60} fullerene [35], B_{80} [36], and BC_3 [4].

Adsorption of Na atom on C_3NNT

The relaxed structures including Na atom are displayed in Fig. 2. After full optimization, Na atom in perfect and

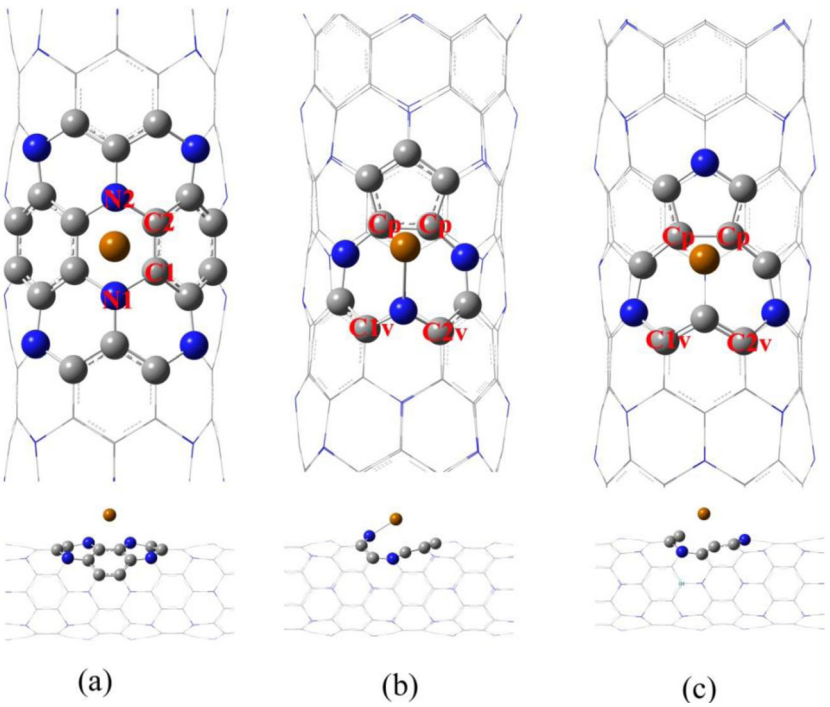

Fig. 2 The optimized structures of Na atom on (**a**) perfect, (**b**) C_v, and (**c**) N_v nanotubes. *Gray*, *blue*, and *brown* colors represent carbon, nitrogen, and sodium atoms, respectively

Table 2 Calculated structural and electronic properties of Na atom on C_3NNT

System	D_{min}(Li-X) (Å)	L (Cp-Cp) (Å)	L (UA-C1v) (Å)	L (UA-C2v) (Å)	E_{gap} (eV)	E_b (eV)	$CT_{(s)}$ |e|	$CT_{(P)}$ |e|	Φ (eV)
Na@perfect	2.392	–	–	–	0.13	−2.054 (−0.83)	−0.86	0.00	1.94
Na@C_v	2.210	1.444	1.390	1.395	0.11	−3.353 (−2.19)	−0.84	0.00	2.03
Na@N_v	2.333	1.505	1.373	1.373	0.04	−2.715 (−1.53)	−0.83	0.00	1.92

Minimum distance of Na atom with nanotube (D_{min}), bond lengths (L), energy gap between valance and conduction bond (E_{gap}), binding energy (E_b), charge transfer of s orbital of Na atom ($CT_{(s)}$), charge transfer of p orbital of Na atom ($CT_{(p)}$), work function (Φ) for Na atom on C_3NNT

defective structures locates on center of hexagon of 4C-2N and nano-membered ring, respectively. As listed in Table 2, D_{min} between Na atom with C atom and N atom in perfect form are 2.753 and 2.392 Å, respectively. Furthermore, D_{min} between Na atom and UA in C_v and N_v structures are 2.210 and 2.333 Å, respectively. The results showed that 0.83, 0.85, and 0.83 |e| are transferred from Na atom to perfect, C_v, and N_v nanotubes, respectively. The calculations showed that E_b of Na atom on perfect, C_v, and N_v structures are −2.05 (−0.83), −3.35 (−2.19), and −2.71 (−1.53) eV, respectively. Since experimental cohesive energy of Na bulk is 1.11 eV/atom [31], clustering of Na atom could be prevented by coating on C_3NNT. In addition, E_b in Table 2 showed that Na atom is satisfied on C_v structure rather than other structures which is consistent with a larger absolute E_b, higher CT, and shorter chemical bonds. Since Na atom on C_3NNT lose more charges and avoids clustering, it can be a good adsorbent for the gas storage applications.

Adsorption of K atom on C_3NNT

The optimized structures of adsorption of K atom on C_3NNT are illustrated in Fig. 3. Like Li and Na atoms, K atom chooses the same positions on the nanotubes. Furthermore, the structural and electronic properties of C_3NNT with K atom are listed in Table 3. D_{min} between K atom with C and N atoms are 3.04 and 2.680 Å, respectively. Moreover, D_{min} of K atoms with surface of C_v and N_v structures are 2.531 and 2.673 Å, respectively. Noteworthy, the distance between the AMs and C_3NNT surface monotonically increases with increasing atomic size. The data from charge analysis on Table 3 showed that due to the hybridization interaction between nanotube and metal atoms, K atoms on the perfect, C_v, and N_v structures lose 0.93, 0.90, and 0.91 |e|, respectively. As reported in Table 3, the E_b of K atoms on perfect, C_v, and N_v structures are −2.52 (−1.31), −3.66

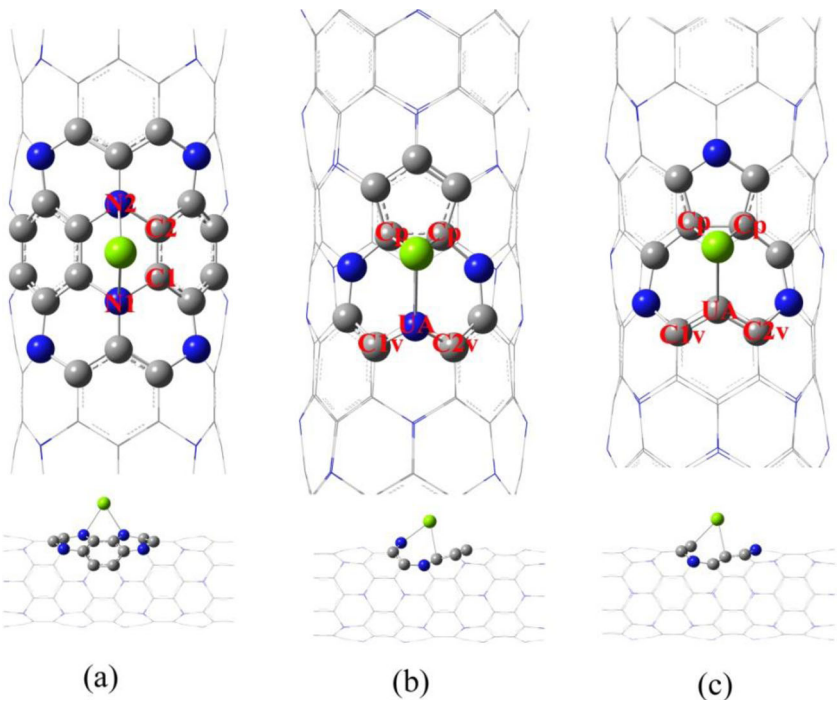

Fig. 3 The optimized structures of K atom on (**a**) perfect, (**b**) C_v, and (**c**) N_v nanotubes. *Gray*, *blue*, and *green* colors represent carbon, nitrogen, and potassium atoms, respectively

Table 3 Calculated structural and electronic properties of K atom on C_3NNT

System	D_{min}(Li-X) (Å)	L (Cp-Cp) (Å)	L (UA-C1v) (Å)	L (UA-C2v) (Å)	E_{gap} (eV)	E_b (eV)	$CT_{(s)}$ |e|	$CT_{(p)}$ |e|	Φ (eV)
K@perfect	2.680	–	–	–	0.08	−2.52 (−1.31)	−0.93	0.00	1.85
K@C_v	2.531	1.436	1.394	1.388	0.11	−3.66 (−2.49)	−0.90	0.00	1.97
K@N_v	2.673	1.499	1.371	1.371	0.05	−3.00 (−1.84)	−0.91	0.00	1.86

Minimum distance of K atom with nanotube (D_{min}), bond lengths (L), energy gap between valance and conduction bond (E_{gap}), binding energy (E_b), charge transfer of s orbital of K atom ($CT_{(s)}$), charge transfer of p orbital of K atom ($CT_{(p)}$), work function (Φ) for K atom on C_3NNT

(−2.49), and −3.00 (−1.84) eV, respectively. Thus, K atom on the C_3NNT has a more E_b respect to cohesive energy of K bulk (0.93 eV/atm) [31]. Therefore, K atom does not suffer from clustering problem. Like Li and Na atoms, C_v structure is the best adsorbent for K atom. Since C_v and N_v structures have UAs, their reactivity with respect to perfect form are expectable. Based upon structural and electronic properties of K atom on C_3NNT, it can be a suitable candidate for gas storage materials.

Electronic structure

Turning now to the chemical nature of the interaction between AMs and the nanotube, the partial density of states (PDOS) of AM@C_3NNT and calculated CT of Li, Na, and K atoms are illustrated in Fig. 4 and Tables 1, 2, and 3, respectively. The results revealed that the AM@C_3NNT complexes are semiconductor with the gaps between 0.04 and 0.13 eV. From CT and the existence of an unoccupied peak of the AMs above the Fermi level, it can be inferred that the AM atom in the system is in a cationic state and can accept electrons from other molecules such as hydrogen molecules. However, like graphene [33], silicene [34], C_{60} [35], and B_{80} [36] there is no clear trend in the adsorption energies. As listed in Tables 1, 2, and 3, the induced positive charge of the AM atoms increases in the order of Li < Na < K, which is very compatible with their reactivity, but inconsistent with the order of their E_b. Such a confliction between the CT and the E_b has also been observed in graphene [33], silicene [34], C_{60} [35], and B_{80} [36]. To continue, we interpret the reason for the above conflict from the electronic structures. As seen in Tables 1, 2, and 3, the Li atom has the highest E_b to the C_3NNT but with a relatively smaller CT. This means that the bonding between the Li atom and the nanotube is different from Na atom and K

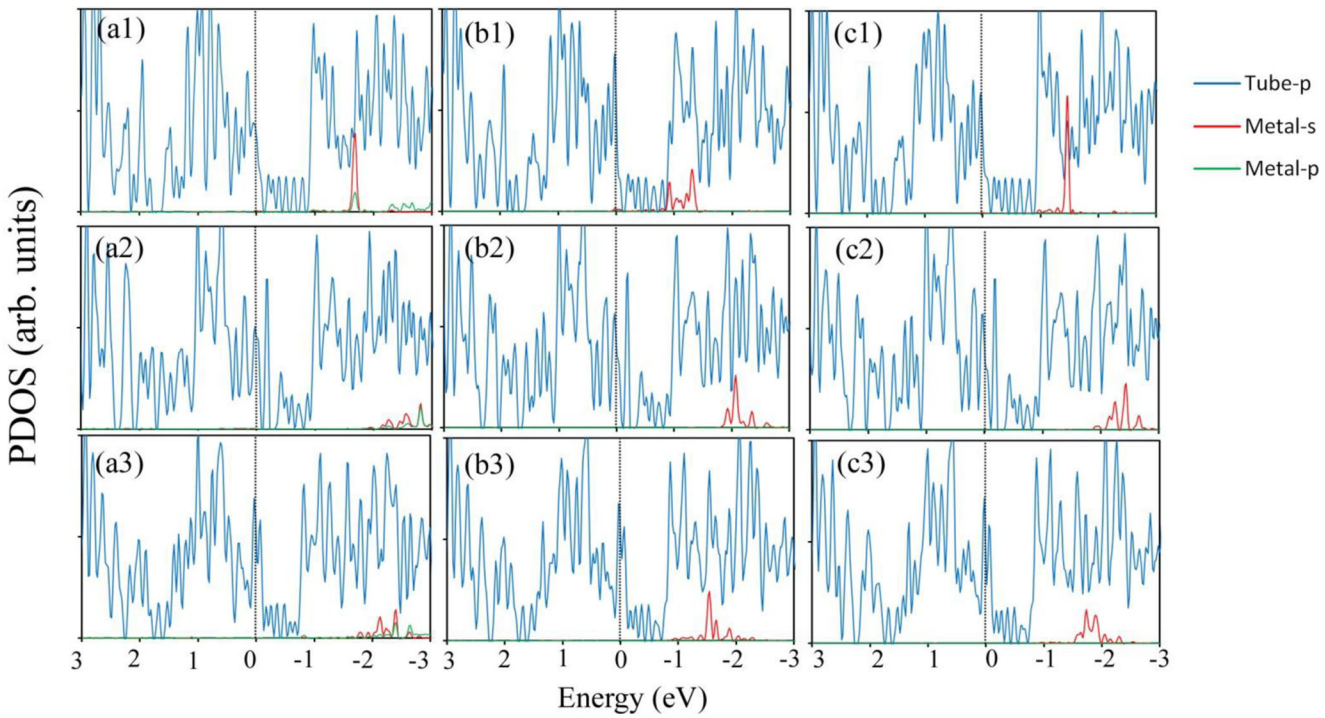

Fig. 4 Partial density of states for (*a1*) Li@perfect, (*a2*) Li@C_v, (*a3*) Li@N_v, (*b1*) Na@perfect, (*b2*) Na@C_v, (*b3*) Na@N_v, (*c1*) K@perfect, (*c2*) K@C_v, (*c3*) K@N_v complexes. The *dashed violet line* indicates the position of Fermi level, which is set to zero energy

atom with nanotube. As interpreted from Fig. 4 and Tables 2 and 3, in the Na- (K-) nanotube complex, the bonding originates from the mixing of the *3s* (*4s*) orbital of Na (K) and *2p* orbital of nanotube, and simultaneously, there exists a CT from the *3s* (*4s*) orbital of Na (K) to the *2p* orbital of nanotube. Therefore, these interactions do not obey Dewar coordination [37]. As indicated in the range of −1.7 eV of Fig. 4a, there is hybridization between *p* orbital of Li and *p* orbital of nanotube. Therefore, *p* orbital of Li participates in the bonding as the Li atom is attached to the nanotube, on the contrary, *p* orbital of Na and K atoms do not participate in the bonding mechanism. From Table 1, as Li atom interacts with the nanotube, 0.87 |e| transfer from s orbital of metal to the nanotube. As revealed in Table 1 and Fig. 4a, the C_3NNT back-donates 0.31 |e| (is obtained by difference of absolute value of charge transfer between *s* and *p* orbitals of Li atom on perfect form) to the *p* orbital of Li, leading to a strong hybridization between *2p* orbital of C atom and N atom with *2p* orbital of Li atom and partial occupancy of *2p* orbital of Li atom. Therefore, this interaction is categorized as Dewar coordination [37]. Thus, the net CT between the Li atom and C_3NNT is quite small. Since hybridization between *p-p* orbitals is stronger than hybridization between *s-p* orbitals, the E_b of the Li atom on the C_3NNT is larger than that of Na and K atoms on C_3NNT. This was also shown in Li-ethylene and Li-B_{80} complexes [36, 38].

As depicted in Tables 1, 2, and 3, the difference in the Fermi level of the defective and non-defective C_3NT in the presence and absence of AM atoms demonstrated a CT between the nanotube and metal atoms in the absorption process. The Φ for perfect, C_v, and N_v nanotubes were obtained 2.35, 2.33, and 2.33 eV, respectively. Interestingly, the results of Tables 1, 2, and 3 revealed that the Li, Na, and K atoms can increase the field emission current of C_3NNT by reducing the Φ. Field emission in semiconductors strongly depends on the Φ [31]. Decreasing the Φ can help the electron emission from the semiconductor surface in the presence of an electric field [31].

Conclusions

Interaction of AMs with perfect and defective (8,0) C_3NNT have been studied using spin polarized density functional theory. Noted that, the distance between the AMs and C_3NNT surface monotonically increases with increasing atomic size. Our study showed that E_b is increased in the order of Li > K > Na. Furthermore, these E_b are obviously much higher than the formation energy of the alkali metal cluster, and hence, one can unquestionably argue that the clustering of the AMs around C_3NNT is not expected. This is an important issue for the study of hydrogen adsorption on the metal-doped nanomaterials. In addition, the chemical nature of interaction between AMs and C_3NNT was studied. Among the AMs, interaction of Li atom with the nanotube can be explained by Dewar model. Interestingly, the results revealed that Li, Na, and K can increase the field emission current of C_3NNT by reducing the work function.

Acknowledgments Computations were performed on the General Purpose Cluster (GPC) supercomputer at the SciNet High Performance Computing (HPC) Consortium. SciNet is funded by: the Canada Foundation for Innovation under the auspices of Compute Canada; the Government of Ontario; Ontario Research Fund − Research Excellence; and the University of Toronto. Further, we are grateful to Sanandaj Branch, Islamic Azad University Council for the financial support of this research.

References

1. Janiak C, Hoffmann R, Sjovall P, Kasemo B (1993) The potassium promoter function in the oxidation of graphite: an experimental and theoretical study. Langmuir 9(12):3427–3440
2. Chen P, Wu X, Lin J, Tan K (1999) High H2 uptake by alkali-doped carbon nanotubes under ambient pressure and moderate temperatures. Science 285(5424):91–93
3. Lan J, Cao D, Wang W, Smit B (2010) Doping of alkali, alkaline-earth, and transition metals in covalent-organic frameworks for enhancing CO2 capture by first-principles calculations and molecular simulations. ACS Nano 4(7):4225–4237
4. Yang Z, Ni J (2012) Li-doped BC3 sheet for high-capacity hydrogen storage. Appl Phys Lett 100(18):183109
5. Yoo E, Kim J, Hosono E, H-s Z, Kudo T, Honma I (2008) Large reversible Li storage of graphene nanosheet families for use in rechargeable lithium ion batteries. Nano Lett 8(8):2277–2282
6. Bruce PG, Freunberger SA, Hardwick LJ, Tarascon J-M (2012) Li-O2 and Li-S batteries with high energy storage. Nat Mater 11(1):19–29
7. Wang Y, Shao Y, Matson DW, Li J, Lin Y (2010) Nitrogen-doped graphene and its application in electrochemical biosensing. ACS Nano 4(4):1790–1798
8. Ayala P, Arenal R, Rümmeli M, Rubio A, Pichler T (2010) The doping of carbon nanotubes with nitrogen and their potential applications. Carbon 48(3):575–586
9. Mabena LF, Ray SS, Mhlanga SD, Coville NJ (2011) Nitrogen-doped carbon nanotubes as a metal catalyst support. Appl Nanosci 1(2):67–77
10. Maldonado S, Morin S, Stevenson KJ (2006) Structure, composition, and chemical reactivity of carbon nanotubes by selective nitrogen doping. Carbon 44(8):1429–1437
11. Jalili S, Molani F, Schofield J (2013) Ti-coated BC2N nanotubes as hydrogen storage materials. Can J Chem 91(999):1–7
12. Pan H, Zhang Y-W, Shenoy VB, Gao H (2011) Metal-functionalized single-walled graphitic carbon nitride nanotubes: a first-principles study on magnetic property. Nanoscale Res Lett 6(1):97
13. Kong XK, Chen QW, Lun ZY (2014) The influence of N-doped carbon materials on supported Pd: enhanced hydrogen storage and oxygen reduction performance. ChemPhysChem 15(2):344–350
14. Reddy ALM, Srivastava A, Gowda SR, Gullapalli H, Dubey M, Ajayan PM (2010) Synthesis of nitrogen-doped graphene films for lithium battery application. ACS Nano 4(11):6337–6342
15. Bu Y, Chen Z, Yu J, Li W (2012) A novel application of g-C_3N_4 thin film in photoelectrochemical anticorrosion. Electrochim Acta 88:294–300

16. Bulusheva L, Okotrub A, Kurenya A, Zhang H, Zhang H, Chen X, Song H (2011) Electrochemical properties of nitrogen-doped carbon nanotube anode in Li-ion batteries. Carbon 49(12):4013–4023
17. Baughman RH, Zakhidov AA, de Heer WA (2002) Carbon nanotubes—the route toward applications. Science 297(5582):787–792
18. Azevedo S, Machado M, Kaschny J (2011) Stability and electronic states of NC3 nanoribbons. Appl Phys A 104(1):55–60
19. Czerw R, Terrones M, Charlier JC, Blase X, Foley B, Kamalakaran R, Grobert N, Terrones H, Tekleab D, Ajayan P (2001) Identification of electron donor states in N-doped carbon nanotubes. Nano Lett 1(9):457–460
20. Hales J, Barnard AS (2009) Thermodynamic stability and electronic structure of small carbon nitride nanotubes. J Phys Condens Matter 21(14):144203
21. Jalili S, Molani F, Akhavan M, Schofield J (2014) Role of defects on structural and electronic properties of zigzag C_3N nanotubes: a first-principle study. Phys E: Low-dimensional Syst Nanostruct 56:48–54
22. Sandré É, Pickard CJ, Colliex C (2000) What are the possible structures for CN_x compounds? The example of C_3N. Chem Phys Lett 325(1):53–60
23. Kim E, Chen C, Köhler T, Elstner M, Frauenheim T (2001) Theoretical study of a body-centered-tetragonal phase of carbon nitride. Phys Rev B 64(9):094107
24. Azevedo S, De Paiva R (2006) Structural stability and electronic properties of carbon-boron nitride compounds. EPL (Europhys Lett) 75(1):126
25. Giannozzi P, Baroni S, Bonini N, Calandra M, Car R, Cavazzoni C, Ceresoli D, Chiarotti GL, Cococcioni M, Dabo I (2009) QUANTUM ESPRESSO: a modular and open-source software project for quantum simulations of materials. J Phys Condens Matter 21(39):395502
26. Perdew JP, Zunger A (1981) Self-interaction correction to density-functional approximations for many-electron systems. Phys Rev B 23(10):5048
27. Perdew JP, Burke K, Ernzerhof M (1996) Generalized gradient approximation made simple. Phys Rev Lett 77(18):3865–3868
28. Vanderbilt D (1990) Soft self-consistent pseudopotentials in a generalized eigenvalue formalism. Phys Rev B 41(11):7892
29. Monkhorst HJ, Pack JD (1976) Special points for Brillouin-zone integrations. Phys Rev B 13(12):5188–5192
30. Löwdin PO (1950) On the non-orthogonality problem connected with the use of atomic wave functions in the theory of molecules and crystals. J Chem Phys 18(3):365–375
31. Kittel C (2005) Introduction to solid state physics, 8th edn. Wiley, New York
32. Zhou Z, Gao X, Yan J, Song D, Morinaga M (2004) A first-principles study of lithium absorption in boron-or nitrogen-doped single-walled carbon nanotubes. Carbon 42(12):2677–2682
33. Chan KT, Neaton J, Cohen ML (2008) First-principles study of metal adatom adsorption on graphene. Phys Rev B 77(23):235430
34. Sahin H, Peeters FM (2013) Adsorption of alkali, alkaline-earth, and 3d transition metal atoms on silicene. Phys Rev B 87(8):085423
35. Chandrakumar K, Ghosh SK (2008) Alkali-metal-induced enhancement of hydrogen adsorption in C60 fullerene: an ab initio study. Nano Lett 8(1):13–19
36. Li Y, Zhou G, Li J, Gu B-L, Duan W (2008) Alkali-metal-doped B80 as high-capacity hydrogen storage media. J Phys Chem C 112(49):19268–19271
37. Mingos DMP (2001) A historical perspective on Dewar's landmark contribution to organometallic chemistry. J Organomet Chem 635(1):1–8
38. Zhou W, Yildirim T, Durgun E, Ciraci S (2007) Hydrogen absorption properties of metal-ethylene complexes. Phys Rev B 76(8):085434